The 1967 Caracas Earthquake: Fault Geometry, Direction of Rupture Propagation and Seismotectonic Implications

GERARDO SUÁREZ

Instituto de Geofísica, Universidad Nacional Autónoma de México, Mexico City

JOHN NÁBĚLEK

College of Oceanography, Oregon State University, Corvallis

The fault plane orientation of the July 30, 1967, Caracas earthquake (M_w=6.6) has been a source of controversy for several years. This strike-slip event was originally thought to have occurred on an east-west oriented fault plane, reflecting the relative motion between the Caribbean and South American plates. More recently, however, the complex seismic radiation from this event was interpreted as being indicative of a north-south striking fault that ruptured along three en echelon segments. In this study we synthesize evidence based on the intensity and damage reports, the distribution of aftershocks, and the results of a joint formal inversion of the P and SH waves and show that these data clearly indicate that the rupture of the 1967 earthquake occurred on an east-west trending fault system. Using a master event technique, the largest aftershock, which occurred 40 min after the main event, is shown to lie 50 km east of the epicenter of the mainshock. The epicentral distances of small aftershocks registered in Caracas, based on the S-P arrival time differences and the polarizations of the P waves, are also consistent with these events occurring on an east-west oriented fault system north of Caracas. A joint inversion of the teleseismic P and SH waves, recorded on long-period seismographs of the World-Wide Standardized Seismographic Network, shows that in a time frame of 65 s, four distinct bursts of seismic moment release (subevents) occurred, with a total seismic moment of 8.6×10^{18} N m. The first three subevents triggered sequentially from west to east, in a direction that is almost identical to the east-west trending nodal planes of the source mechanisms. The average depth of these three subevents is 14 km. The fourth, and last identifiable, subevent of the sequence shows a reverse faulting mechanism with the nodal planes oriented roughly east-west. It occurred at a 21-km depth, about 50 km to the north of the fault zone defined by the strike-slip subevents. This fourth subevent appears to reflect compressional deformation of the southern Caribbean, possibly related to underthrusting along the proposed Curaçao trench. The complexity of the fault system causing the 1967 earthquake suggests that the relative motion along the Caribbean-South America plate boundary in central Venezuela is taken up over a broad, highly faulted, and highly stressed zone of deformation and not by a simple, major throughgoing fault.

INTRODUCTION

On July 30, 1967, parts of the city of Caracas and several neighboring coastal towns were severely damaged by a moderate-sized earthquake (M_w=6.6). Although the so-called Caracas earthquake was not a great plate boundary earthquake, it is one of the largest event to have occurred along the Caribbean-South American plate boundary in central Venezuela since the magnitude 8.4 (M_s) earthquake of 1900 [*Richter*, 1958]. Thus the Caracas earthquake represents an important piece of evidence for understanding the tectonic regime and seismic hazard of this complex plate boundary.

The fault plane solution of the Caracas earthquake based on P wave first motions [*Molnar and Sykes*, 1969] shows a nearly pure strike-slip mechanism with nodal planes oriented N10°W and N80°E, respectively. *Molnar and Sykes* [1969] originally interpreted this earthquake as occurring on an east-west trending, right-lateral strike-slip fault, reflecting the relative motion between the Caribbean and South American plates. *Rial* [1978], however, suggested, on the basis of body wave modeling, that the Caracas earthquake occurred on a series of en echelon faults striking north-south and with a left-lateral motion. *Rial* [1978] reached his conclusion based on the interpretation of the asymmetry in the observed waveforms.

Although the tectonic fabric in north central Venezuela is dominated by a series of right-lateral strike-slip faults oriented roughly east to west [*Rod*, 1956; *Schubert*, 1981; *Soulas*, 1986] (Figure 1), the region near Caracas exhibits a complex faulting pattern including faults oriented in a NNW-SSE direction (Figure 2). This complexity may be related to the bend in the plate boundary that takes place in the vicinity (Figure 1). The motivation for reanalizing the Caracas earthquake comes from the observation that although rupture on faults oriented north-south is quite feasible in this tectonically complex area, the solution proposed by *Rial* [1978] does not explain adequately the intensity distribution and damage, nor the location of aftershocks.

Furthermore, aside from being an important datum in an area of low background seismicity and of relatively short seismic history, the Caracas earthquake is also a peculiar and particularly interesting earthquake from the point of view of seismic rupture propagation. As *Rial* [1978] pointed out, the rupture process of this earthquake is very complex. The body wave trains last up to 100 s, almost 5 times as long as would be expected for a shallow earthquake of that magnitude, and show several distinct subevents. The study by *Rial* [1978] is of particular interest because it represents the first attempt to use body wave modeling in order to investigate the rupture process of a complex event.

The purpose of this work is to further the study of the 1967 earthquake initiated by *Rial* [1978]. In order to characterize the time history and geometry of the rupture process, we
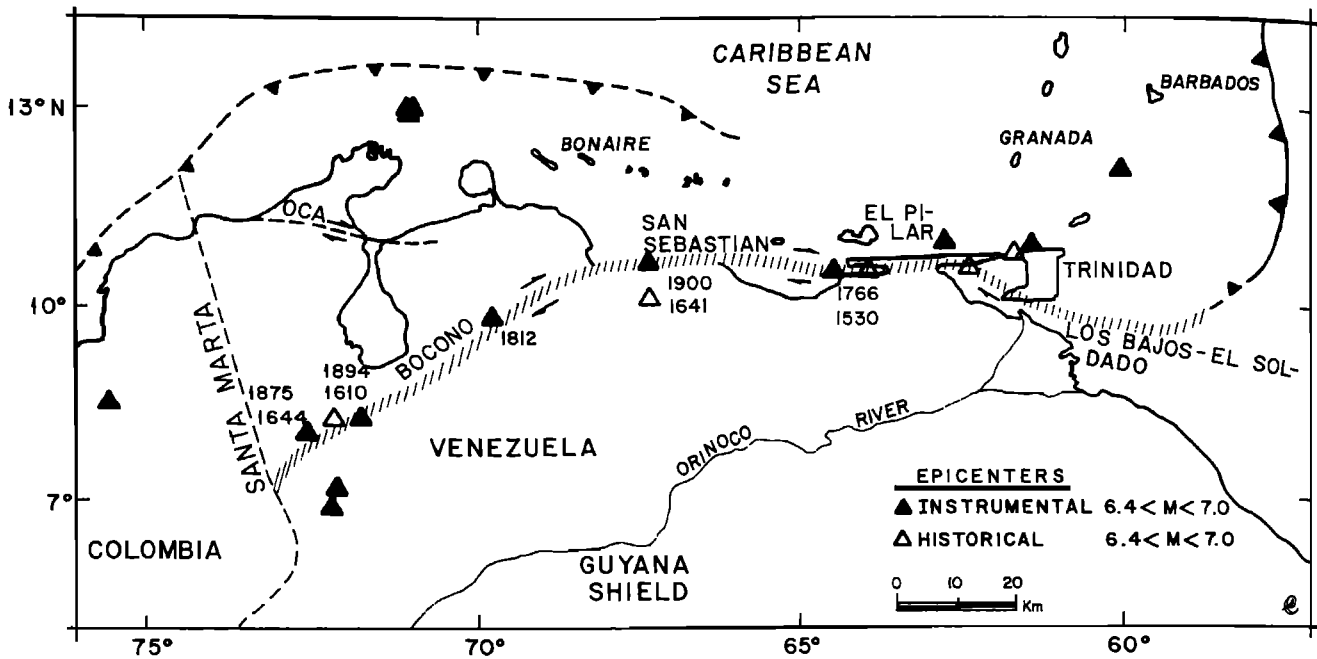
Fig. 1. Regional seismotectonic setting of the southern Caribbean. The main fault zones accommodating the motion of the South American plate relative to the Caribbean are shown. The dates on the faults are of large historical earthquakes. The subduction zone to the north of Bonaire and Los Roques is that inferred by *Talwani et al.* [1977] (modified after Y. P. Aggarwal (personal communication, 1987)).

synthesize evidence from the damage and intensity reports, the epicentral location of the mainshock, the distribution of aftershocks, and the geologic information. Furthermore, we present a detailed study of the body waves using a formal least squares inversion algorithm [*Nábělek*, 1984]; this deterministic approach eliminates many of the resolution problems encountered in a trial-and-error, visual matching of the observed and synthetic waveforms. The main conclusion of our study is that, contrary to *Rial*'s [1978] initial suggestion, the 1967 earthquake occurred on a set of east-west trending fault planes.

TECTONICS AND SEISMICITY OF NORTHERN VENEZUELA

Regional Plate Tectonic Setting

The tectonic structure of northern Venezuela reflects a complex geodynamic regime in which the major geologic features are a consequence of the relative plate motion between the South American and Caribbean plates [*Barazangi and Dorman*, 1969; *Burke et al.*, 1984; *Dewey*, 1972; *Molnar and Sykes*, 1969; *Schubert*, 1981, 1984; *Schubert and Krause*, 1984; *Sykes and Ewing*, 1965] (Figure 1). The Caribbean plate moves to the east relative to the South American plate [*Jordan*, 1975; *Minster and Jordan*, 1978; *Stein et al.*, 1988]. East of the island of Trinidad, the plate boundary changes from a subduction regime in the Lesser Antilles, to a system of right-lateral strike-slip faults. *Pérez and Aggarwal* [1981] suggest that the Los Bajos-El Soldado fault system (Figure 1) defines the plate boundary between the Lesser Antilles subduction zone and the Paria Peninsula in Venezuela. West of the Paria Peninsula, the right-lateral strike-slip system extends over 1200 km and is subdivided into three major fault zones: El Pilar, Moron, and Bocono (Figure 1). The width of major tectonic deformation along this fault system is of the order of 100 km [*García and Aggarwal*, 1982; *Soulas*, 1986].

On average, the background seismicity along this plate boundary is low, probably due to the low relative velocity between the two plates. Nonetheless, large historical earthquakes have occurred along various segments of this fault system [*Centeno-Grau*, 1940]. Great earthquakes probably occurred on the El Pilar fault in 1530 and 1766 [*Centeno-Grau*, 1940; *Grases*, 1980], and the great earthquake of 1812 caused destruction along the Bocono and Moron faults, from Merida to Caracas (*Fiedler* [1961] mapped intensity IX in both cities).

Active Faults in North Central Venezuela

The Moron fault zone that presumably defines the plate boundary between the Caribbean and South American plates in central northern Venezuela, near Caracas, is not a single, well-defined strike-slip fault but is a system of en echelon, right-lateral faults, oriented roughly east-west [*Rod*, 1956; *Schubert and Krause*, 1984; *Soulas*, 1986] (Figure 2). Moreover, there are some faults with a NW-SE trend showing both strike-slip and normal faulting [*Schubert and Laredo*, 1979; *Singer*, 1977] (Figure 2). The complexity and segmentation of the plate boundary in this region, compared to the more linear and well-defined faults to the east (El Pilar fault) and to the SW (Bocono fault), probably is a consequence the sharp change in strike (about 45°) between these two major fault zones (Figure 1). Although the apex of the bend is presumed to be about 100 km west of Caracas, it is expected that the deformation produced by the bend would cover a large area.

The two largest, recent earthquakes to have occurred in north central Venezuela are the 1967 Caracas earthquake and an event on October 29, 1900, for which *Richter* [1958] estimated a magnitude of 8.4. As *Kelleher et al.* [1973] pointed out, it is difficult to establish which segment of the fault system is responsible for the 1900 earthquake. The instrumental epicenter determined by *Richter* [1958] lies 100 km to the east of the area of maximum intensity (around Caracas) reported by *Fiedler* [1961]. Furthermore, the magnitude appears to be
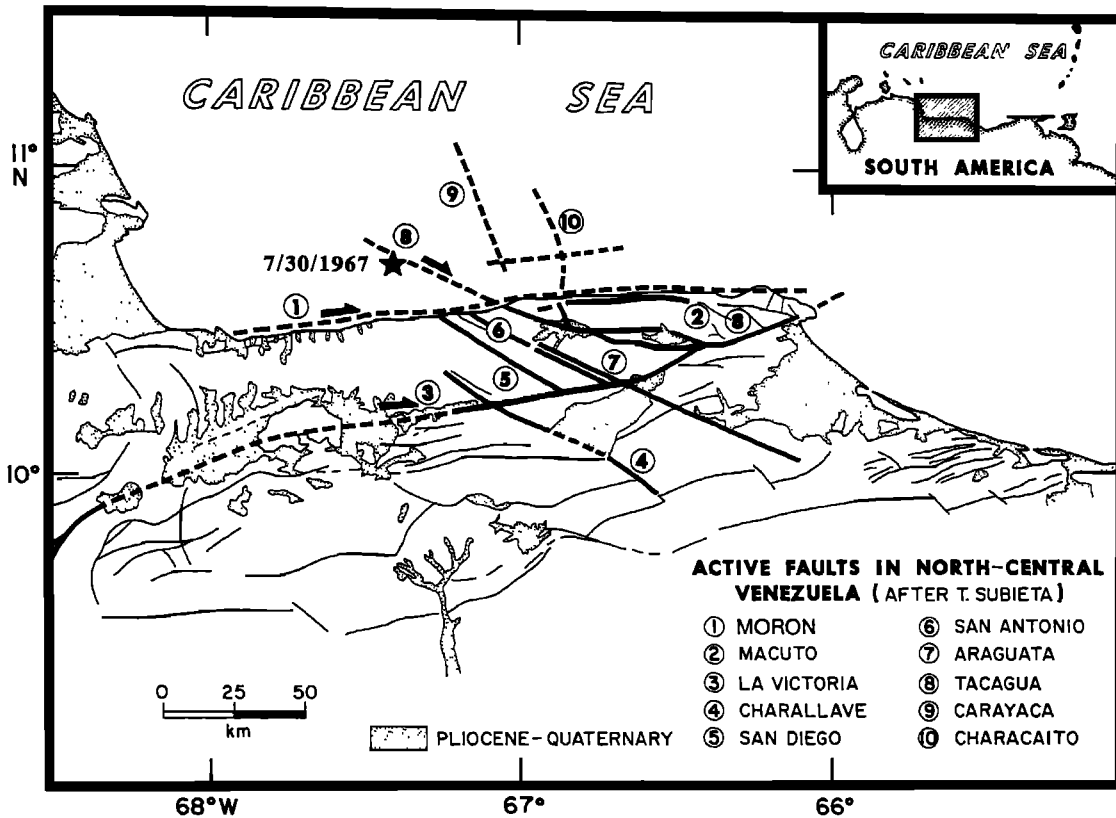
Fig. 2. Geologic faults presumed to be active in north-central Venezuela (modified after *Subieta* [1983]). Solid lines indicate mapped faults and dashed lines inferred faults. Stippled regions indicate presence of Pliocene and Quaternary sediments. The star marks the epicenter of the 1967 Caracas earthquake.

largely overestimated considering that the zone of intensity IX to X is only about 50 km long [*Cisternas and Gaulon*, 1984; *Fiedler*, 1961]. Based on the intensity reports, it is possible that the rupture of the 1900 earthquake included some of the same fault segments as the 1967 event. The only other major historical earthquake that occurred in this region besides the 1812 and 1900 earthquakes is an earthquake in 1641 [*Centeno-Grau*, 1940]. The fact that no great earthquakes have occurred along this plate boundary during the last 87 years highlights the importance of the 1967 Caracas earthquake.

EPICENTER, INTENSITY REPORTS, AND AFTERSHOCK
DISTRIBUTION: IMPLICATIONS FOR
THE FAULT ORIENTATION

Epicentral Location of the Mainshock

The epicenter of an earthquake, being determined from arrival times of short-period body waves, reflects the location of the point on the fault plane where rupture initiates. Usually, when an event with a complex fault rupture process is studied using the shape and duration of the body waves, the locations of the subevents that compose the earthquake are estimated relative to the point of nucleation of the rupture (the epicenter). A good estimate of the epicenter is necessary for geographical placement of the subevents. As we discuss below, in the case of the Caracas earthquake, the choice of the epicenter is also crucial for the interpretation of the intensity data and the distribution of aftershocks.

The model derived by *Rial* [1978] from waveform modeling is composed of three en echelon faults oriented NNW-SSE that ruptured sequentially from north to south (Figure 3). Rial

places this fault system so that it passes through Caracas and would, at the first glance, adequately explain the damage and intensities reported by *Espinosa and Algermissen* [1972] and those we obtained by reviewing accounts of the earthquake in various Venezuelan journals and magazines (Figure 4). To place this fault system geographically, Rial uses a preliminary epicentral location determined by *Fiedler* [1968]. The location proposed by *Fiedler* [1968] lies 70 km offshore NNW of Caracas. It was obtained by measuring the arrival time differences of P_n waves at various pairs of seismic stations in the Caribbean basin. The epicenter was determined graphically as the intersection of the epicentral distance hyperbolae for the individual station pairs. In spite of drastically different propagation paths, *Fiedler* [1968] assumed that the velocity of the P_n phase is the same for all stations. Given the assumptions used, this graphical method gives only a rough estimate of the epicenter.

The epicenter obtained by *Fiedler* [1968] is located about 40 km to the NE from that determined by the International Seismological Center (ISC) (Figure 3). The epicentral locations reported by the ISC, the U.S. Coast and Geodetic Survey, and Moscow show differences of less than 10 km among them. The teleseismic station coverage of the southern Caribbean is good, and the errors in epicentral locations are generally less than about 15 km for earthquakes greater than magnitude 5.0 that are well recorded worldwide. This observation is confirmed by comparing the epicentral locations obtained by the ISC and by a local network in Venezuela (installed after the 1967 earthquake), for 15 earthquakes selected at random (Figure 5). For these earthquakes, all smaller than the 1967 event, the differences in epicentral locations between those obtained
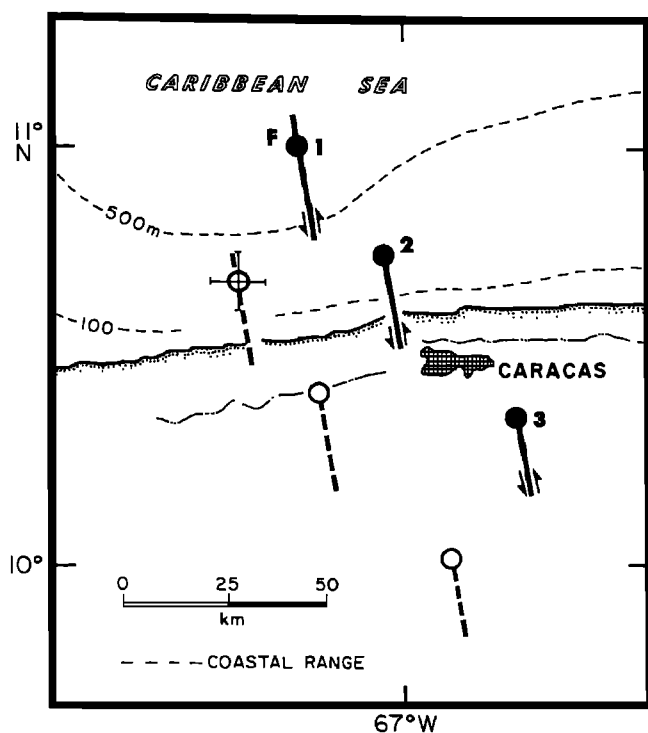
Fig. 3. Location of the subevents (solid circles) and the north-south trending fault system (solid lines) proposed by *Rial* [1978]. The location of the first subevent is made to coincide with the preliminary epicenter determined by *Fiedler* [1968] (marked F). The open circles and dashed lines indicate the location relative to the epicenter determined by the International Seismological Center (ISC). Note that when the fault system is located relative to the more precise ISC location (error bars shown), it lies well to the south and west of Caracas.

using local instruments and the worldwide network are usually less than 15 km; only three small events ($m_b < 4.0$) show differences of 30–35 km. We believe that 40-km distance between the location proposed by *Fiedler* [1968] and that of the ISC reflects primarily the inaccuracy of the method used by the former.

Intensity Distribution and the Orientation of the Fault System

The choice of the epicenter is crucial for the model proposed by *Rial* [1978], because when the fault system is moved to the more precise ISC epicentral location, his proposed faults lie about 60 km to the west and south of Caracas. With the faults at this location (Figure 3), it is difficult to explain the observed intensity data (Figure 4). The regions that experienced damage and high intensities are located near Caracas and along the coast immediately to the north of the capital. If isoseismal curves were drawn on Figure 4, they would show a semicircular distribution centered roughly north of Caracas, with intensities gradually decreasing away from the city. It is difficult to explain how cities like Maracay, Turmero, and Valencia, for example, that lie at a similar distance from the fault system defined by *Rial* [1978] as Caracas and are located also on loosely consolidated sediments (Figure 2), consistently show intensities three to four degrees lower than those reported at the north coast of Caracas.

In fact, no matter which epicenter is used to geographically place *Rial*'s [1978] north-south trending fault system, it is difficult to explain the absence of high intensities south of Caracas, in the towns of Cua, Ocumare del Tuy, and Santa

Teresa, among others (Figure 4). Particularly large accelerations would be expected in this region, because it lies within 10–15 km away from the third segment in a north-south oriented fault system, which in Rial's model had the highest moment release. On the other hand, faulting along the nodal plane striking almost east-west to the north of Caracas (dashed thin line in Figure 4) would explain the high intensities observed in and to the north of Caracas ($\geq$VI) and the smaller values ($\leq$ V) observed in towns to the west and south of the city (Figure 4).

Although intensity information is missing from the regions to the west and southwest of Caracas because these areas are largely uninhabited, there is sufficient information available indicating that the largest intensities occurred north of Caracas along the Caribbean coast, with intensity decreasing southward from the coast. Local ground amplification due to unconsolidated sediments was possibly responsible for the localized damage to high-rise buildings in Caracas [*Espinosa and Algermissen*, 1972; *Seed et al.*, 1970; *Whitman*, 1969], but the distribution of Quaternary deposits (Figure 2) shows that this factor alone cannot reconcile the observed damage and intensity distribution with the fault system proposed by *Rial* [1978]. The construction of low-rise housing is fairly uniform throughout the area and provides a good measure of variations in intensity (and acceleration) in the macroseismic zone. The damage sustained by this type of constructions is higher along the coast north of Caracas than it is elsewhere.

Spatial Distribution of Aftershocks

The most direct way for determining the orientation of an earthquake rupture, other than actually mapping its surface expression, is from the distribution of aftershocks. The Caracas earthquake, however, had no large enough aftershocks that were well recorded by the worldwide seismic networks, and the local seismographs in Caracas capable of recording smaller events were damaged for a few days after the earthquake. It is remarkable that an earthquake of the magnitude of the Caracas event, and with such complex history and geometry of rupture, did not produce larger aftershocks.

The only suggestion for a moderately large aftershocks comes from newspaper accounts describing other strong quakes shaking the city of Caracas after the mainshock. The largest of these aftershocks caused panic among the population and occurred about 40 min after the main event. The ISC reports this event as occurring offshore at a depth of 114 km. The location is poor because the magnitude of this earthquake ($m_b = 4.4$) is near the threshold of detection for earthquakes in this region by the worldwide networks and the local stations were not operating. It was possible, however, to identify clear first arrivals of the aftershock on several stations in the Caribbean (Table 1). We relocated the aftershock relative to the mainshock using the master event technique of *Dewey* [1971].

The relocated epicenter of the aftershock lies 50 km to the east of the mainshock's epicenter, at a focal depth of 10 km, and about 10 km offshore (Table 2 and Figure 6). The location near Caracas explains why this relatively small aftershock ($m_b = 4.4$) was so strongly felt and "heard" in Caracas and the coastal towns. The location of the largest aftershock to the east of the mainshock epicenter strongly suggests a fault extending east-west, north of Caracas.

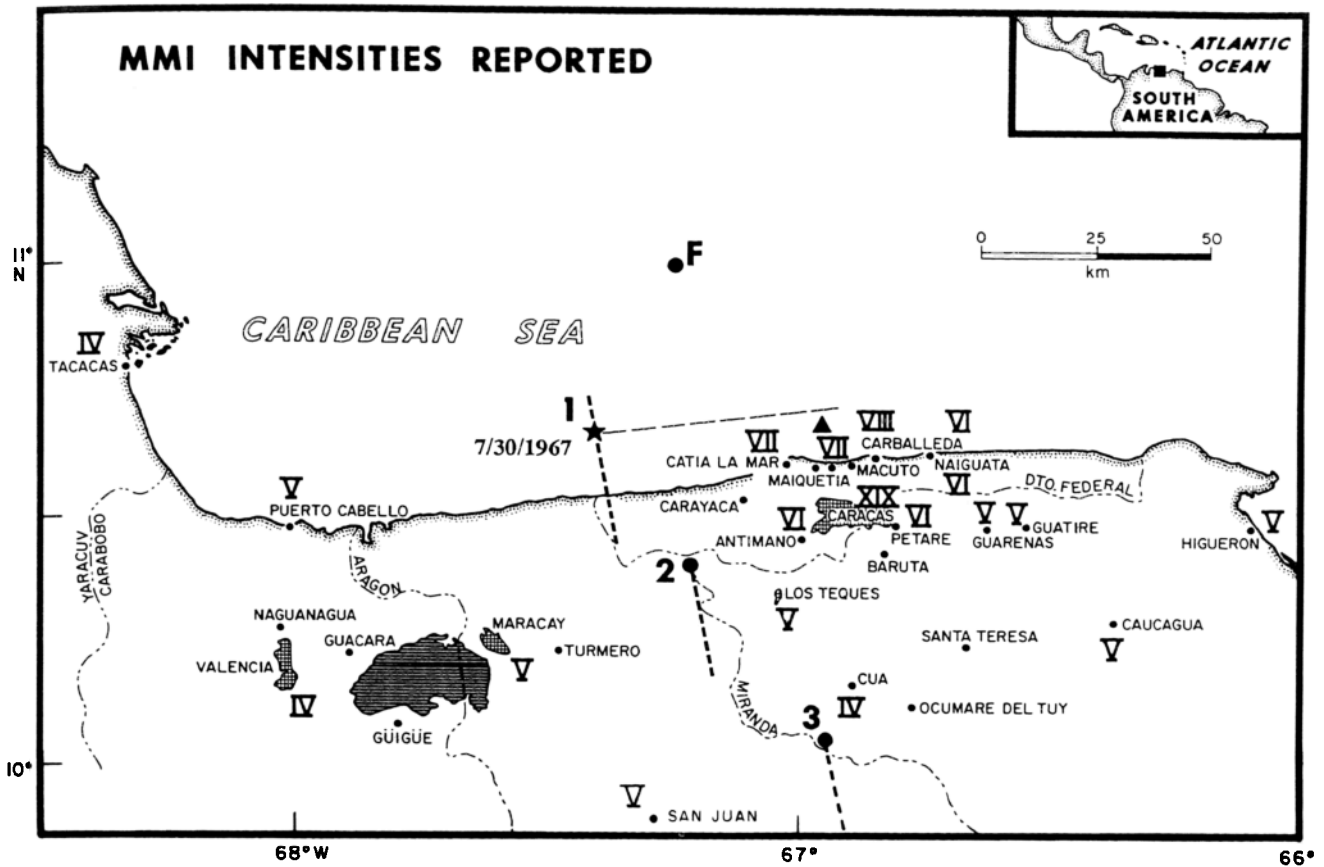The short-period instruments at station CAR (Caracas), member of the World-Wide Standardized Seismographic

Fig. 4. Modified Mercalli intensities (MMI) observed in central Venezuela during the 1967 earthquake. The data come from the study of *Espinosa and Algermissen* [1972] and from our own readings of Venezuelan journals, magazines, and government reports. F marks the location of the preliminary epicenter determined by *Fiedler* [1968]. The short-dashed lines indicate the fault system proposed by *Rial* [1978], located relative to the epicenter determined by the ISC (star). The long-dashed line shows the strike of the east-west nodal plane of the focal mechanism.

Network (WWSSN), became again operational a fews days after the earthquake occurred. Dozens of small aftershocks were recorded at CAR in the following month. Although epicentral locations of these small aftershocks cannot be obtained with only one station, it was possible to identify in the original records clear compressional (P) and shear wave (S) phases. Measuring the S-P travel time differences, the epicentral

Fig. 5. Histogram showing differences in epicentral location for 15 earthquakes located by a local seismic network in Venezuela and by the ISC.

distance from the recording station may be estimated and plotted on a map (Figure 7).

Assuming the rupture nucleated near the ISC epicenter, most of the 22 aftershocks analyzed would fall well to the east of the proposed north-south fault system (Figure 7). Clearly, the epicentral distances of the aftershocks to station CAR would agree better with an east-west oriented fault north of Caracas, as most of the epicentral distance radii intersect the line representing the east-west nodal plane of the focal mechanism (Figure 7). Furthermore, based on the polarization of the P waves from the aftershocks that were well recorded both on the vertical and horizontal instruments at station CAR, it is clear that all of them have a location to the north and northwest of CAR.

The results presented above strongly favor the initial assumption of *Molnar and Sykes* [1969] that the Caracas earthquake occurred on one of the various east-west running faults that define this complex plate boundary. This prompted us to reexamine quantitatively the radiation of P and SH waves using a formal inversion scheme. The following section describes the results of this analysis.

INVERSION OF BODY WAVES

Data Preparation and Inversion Method

The source parameters and rupture process of the Caracas earthquake are investigated through an inversion of long-period P waves and SH waves recorded by the WWSSN. Only
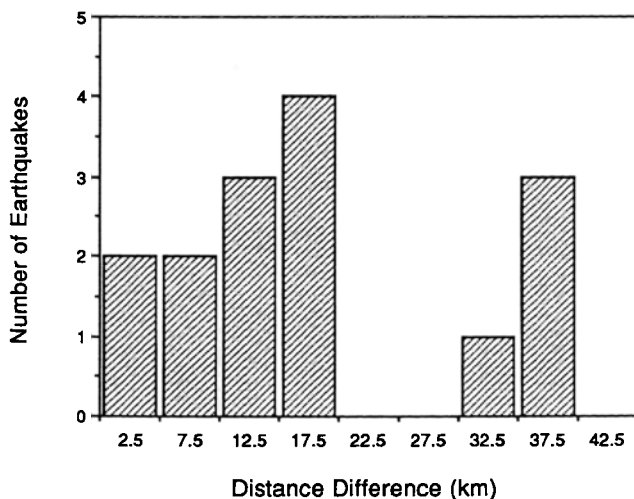
TABLE 1. Stations Used in the Relocation of the Aftershock

Station Name	Arrival Time of P Wave, GMT
TRN	0041:02.5
SVT	0041:08.4
SJG	0041:27.7
BOG	0041:56.5
HUA	0044:58.0
PNS	0045:29.2
LPB	0045:27.3
WMO	0046:57.8
TFO	0048:09.4
LF2	0048:27.8
BMO	0049:18.4
ILG	0050:50.8

seismograms of stations within an epicentral distance range of 30°–90° were included in the analysis; within this distance range, the Green functions for a source embedded in a layered earth are simple to compute and can be accurately estimated [e.g., *Langston and Helmberger*, 1975]. The crustal structure in the source region and beneath recording stations was approximated by a half-space with a compressional wave velocity of 6 km/s, a Poisson ratio of 0.25, and density of 2.75 g/cm³. Anelastic attenuation along the propagation path was parameterized using a t^* of 1 s for P waves and a t^* of 4 s for SH waves.

The inversion procedure is discussed in detail by *Nábělek* [1984] and has been applied succesfully to other large earthquakes [*Nábělek*, 1985; *Nábělek* et al., 1987]. Depending on the size and complexity of the earthquake, the source can be parameterized either as a single point source or as an event consisting of several point sources (subevents) separated in

TABLE 2. Focal Parameters of the Mainshock and the Relocated Aftershock

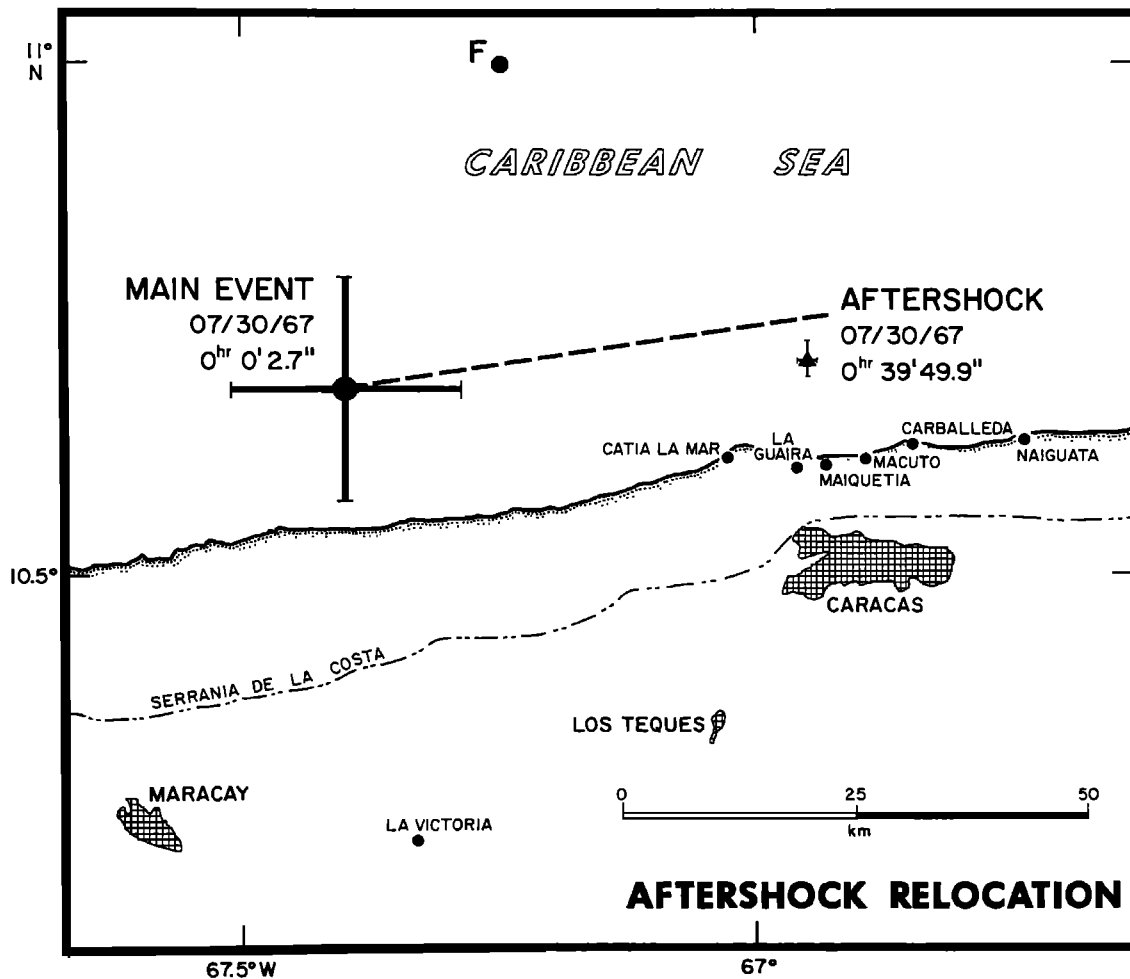| Date	Origin Time, GMT	Latitude, °N	Longitude, °W	Depth, km	Source
July 30, 1967	0000:02.7	10.68	67.40	26	ISC
July 30, 1967	0039:49.9	10.70	66.95	10	this study

Fig. 6. Master event relocation of the largest aftershock (solid triangle) felt in the Caracas region about 40 min after the mainshock (solid circle). The mainshock was used as the master event in the relocation. The lines through these symbols are error estimates of the location. The dashed line shows the orientation of the nodal plane oriented east-west.
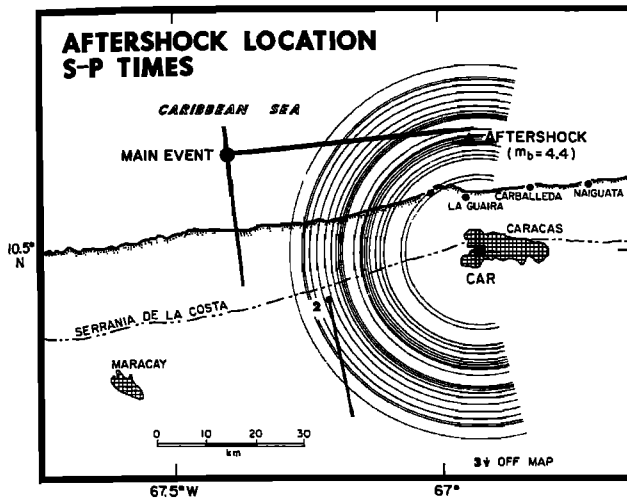
Fig. 7. Circles of possible epicentral locations of small aftershocks relative to station CAR. The epicentral distances are based on readings of *S-P* travel time differences. Other symbols are as in Figure 6.

time and space. For each subevent, the model parameters that we invert for from the observed seismograms include the source mechanism (strike, dip, and rake), depth, seismic moment, source time function, and the relative location and time delay of each subevent with respect to the first one. The source time function is allowed to take an arbitrary shape, making the parameterization suitable for studies of large, complicated earthquakes. The data used in the inversion are hand-digitized time series (two samples per second) of the observed P (vertical component) and SH seismograms, in a time window that includes the direct body wave phases and extends in time to include all surface reflected waves (i.e., pP, sP, and sS). The seismic phases and stations used in the inversion are shown in Table 3. Theoretical seismograms are iteratively matched to the observed waveforms using a least squares criterion.

Visual Comparison of Waveforms

Before proceeding to the formal inversion of the data, it is instructive to visually compare the waveforms at several stations to ascertain directly if substantial differences exist in the shape of the body waves that would suggest directivity of the source rupture process. For this purpose, we compare the body waves recorded at three east-west and north-south pairs of seismic stations located symmetrically relative to the nodal planes of the fault plane solution of the Caracas earthquake (Figure 8). For a pure strike-slip event, this symmetric location relative to the source mechanism insures that the waveforms have a similar location relative to the radiation pattern of direct and reflected phases. The polarities have been made the same for each pair of stations in order to facilitate the direct visual comparison. Thus for each pair of stations the waveforms may be directly compared, and any drastic differences in waveforms should reflect the effects of rupture directivity and source finiteness.

The P waves recorded at station MAL (Spain) are more compressed in time than those observed at station UNM (Mexico). The first two peaks are almost in phase, but the third and largest peak is clearly delayed at UNM relative to its counterpart at MAL. Subsequent peaks and troughs in the signals show a much longer, low-frequency signal at UNM than at MAL (Figure 8). This observation is even more apparent comparing SH waveforms recorded at TOL (Spain) and KIP (Hawaii). At TOL the observed SH waves are compressed, exhibiting a much shorter duration than at KIP (Figure 8). These two sets of stations, located roughly to the east and west of the epicenter, suggest a rupture propagating from west to east; the receding rupture front produces long-duration signals at stations to the west of the epicenter, while those to the east, lying along a similar azimuth as the direction of rupture, are strongly compressed.

The SH waves recorded at CMC (Canada) and LPA (Argentina), seismic stations located to the north and south of the epicenter, respectively, are very similar to one another. The prominent peaks and troughs of both time series are in phase, and the duration of the signal is almost identical in both cases. We interpret this as evidence that no major directivity occurred in the north-south direction. No north-south, P wave pair is presented because of the lack of long-period P wave data to the south of the epicenter in the 30°–90° epicentral distance range.

TABLE 3. Seismic Stations Used in the Inversion of Body Waves

Station	Azimuth, deg	Epicentral Distance, deg	Wave Type	Network
GDH	5.7	59.2	P	WWSSN
KEV	20.5	81.6	P	WWSSN
COP	35.1	75.5	P	WWSSN
MAL	54.1	62.1	P	WWSSN
UNM	289.5	31.8	P, SH	WWSSN
LUB	311.3	38.9	P	WWSSN
OXF	323.2	31.1	P	WWSSN
COL	334.4	76.3	P	WWSSN
RES	352.3	65.9	P	CSN
SCH	0.5	44.1	SH	CSN
ESK	34.1	66.7	SH	WWSSN
TOL	50.6	62.8	SH	WWSSN
LPA	169.2	46.3	SH	WWSSN
PEL	184.0	43.8	SH	WWSSN
KIP	291.1	86.7	SH	WWSSN
GOL	317.3	44.4	SH	WWSSN
CMC	342.0	65.1	SH	CSN

EAST   P MAL   EAST   SH TOL   NORTH   SH CMC

WEST   P UNM   WEST   SH KIP   SOUTH   SH LPA
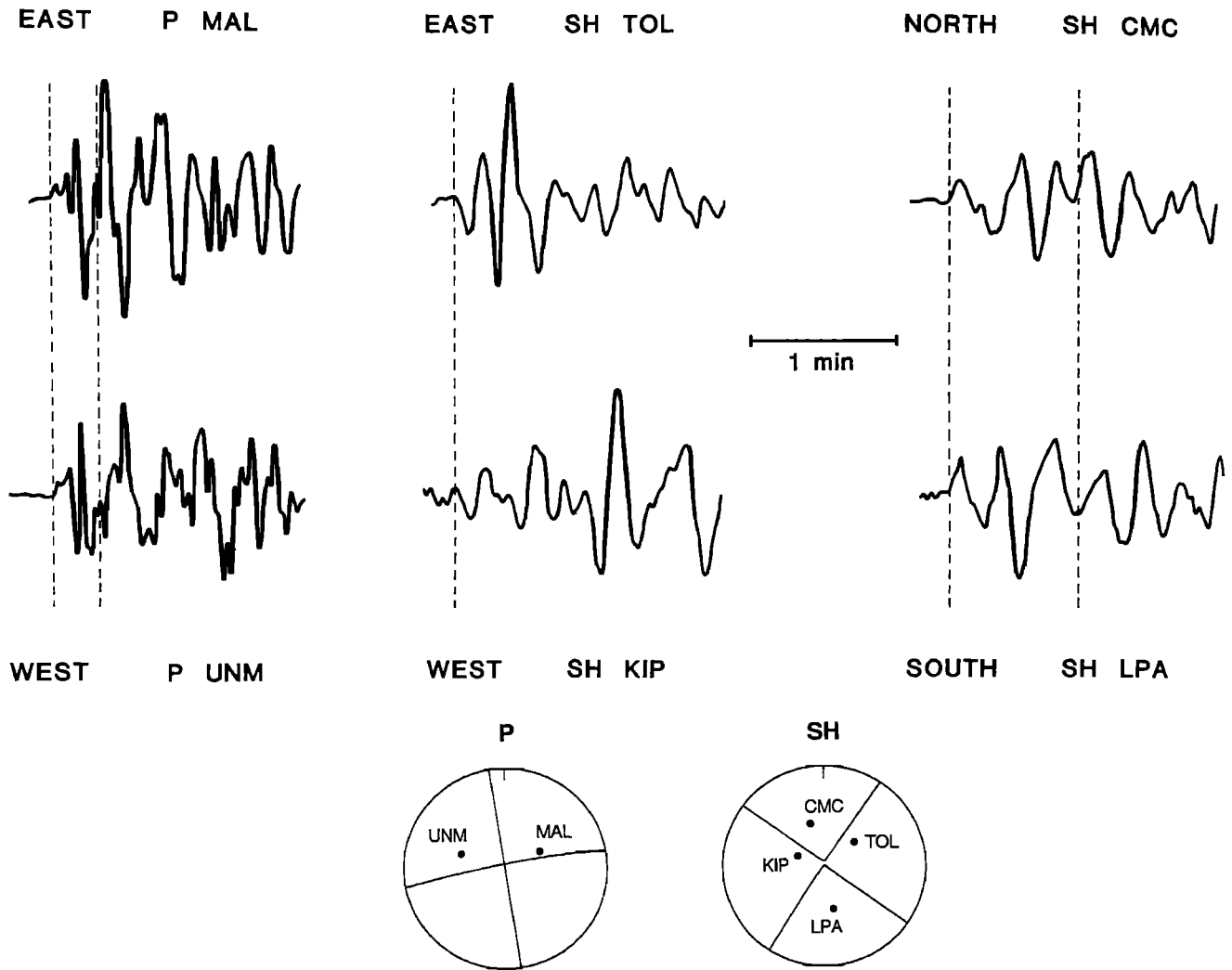
P   SH

Fig. 8. Comparison of *P* and *SH* waves located symmetrically with respect to the focal mechanism of the Caracas earthquake. Notice how stations to the east (TOL and MAL) show a more compressed wavetrain than those to the west (UNM and KIP). *SH* waves to the north and south of the epicenter (CMC and LPA) do not show major differences suggesting the rupture process had an east-west propagation. The ray paths to the stations and the nodal planes are projected of the lower part of the focal sphere.

Inversion Strategy

The waveforms indicate that the Caracas earthquake is a complex, multiple event. *Rial* [1978] showed that at least three subevents were necessary to match the observed wave trains. The number of free source parameters necessary to describe these waveforms is quite large. To deal with the complexity of the source mechanism, while trying to keep the number of free parameters to a minimum, a stepwise inversion strategy was adopted. As a first step, the Caracas earthquake was assumed to be a single-point source with a long source time function. The starting source mechanism for the inversion was that of *Molnar and Sykes* [1969]. This inversion gave the average (centroidal) mechanism with a strike of 262°, dip of 74°, and a rake of 183° and showed that four subevents are needed to model the rupture. Next, in order to determine the predominant direction of rupture propagation, we introduced the effect of rupture directivity into the model [*Nábělek*, 1984, 1985] and varied the rupture direction as a function of azimuth; here we assumed the rupture velocity of 2.4 km/s and used the above source mechanism. The resulting plot of residual variance versus azimuth is displayed in Figure 9, showing a variance reduction of about 30% along the
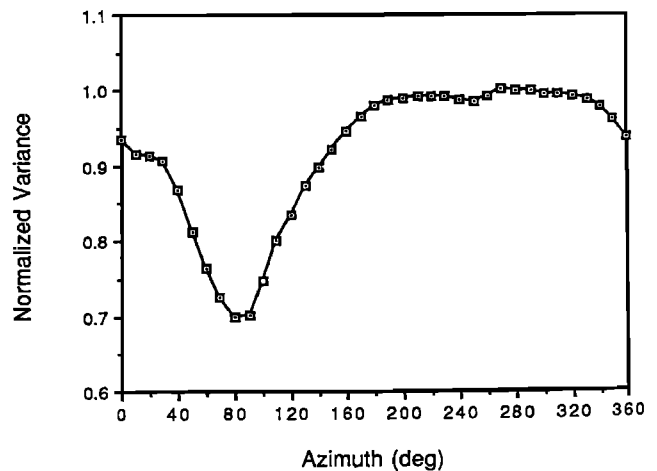
Fig. 9. Variance of the residuals as a function of azimuth of the rupture propagation direction for an unilaterally propagating source with a velocity of 2.4 km/s. The clear variance minimum indicates that the rupture of the Caracas earthquake propagated predominantly along an azimuth of 80°. The average mechanism and depth given in Table 4 are used.
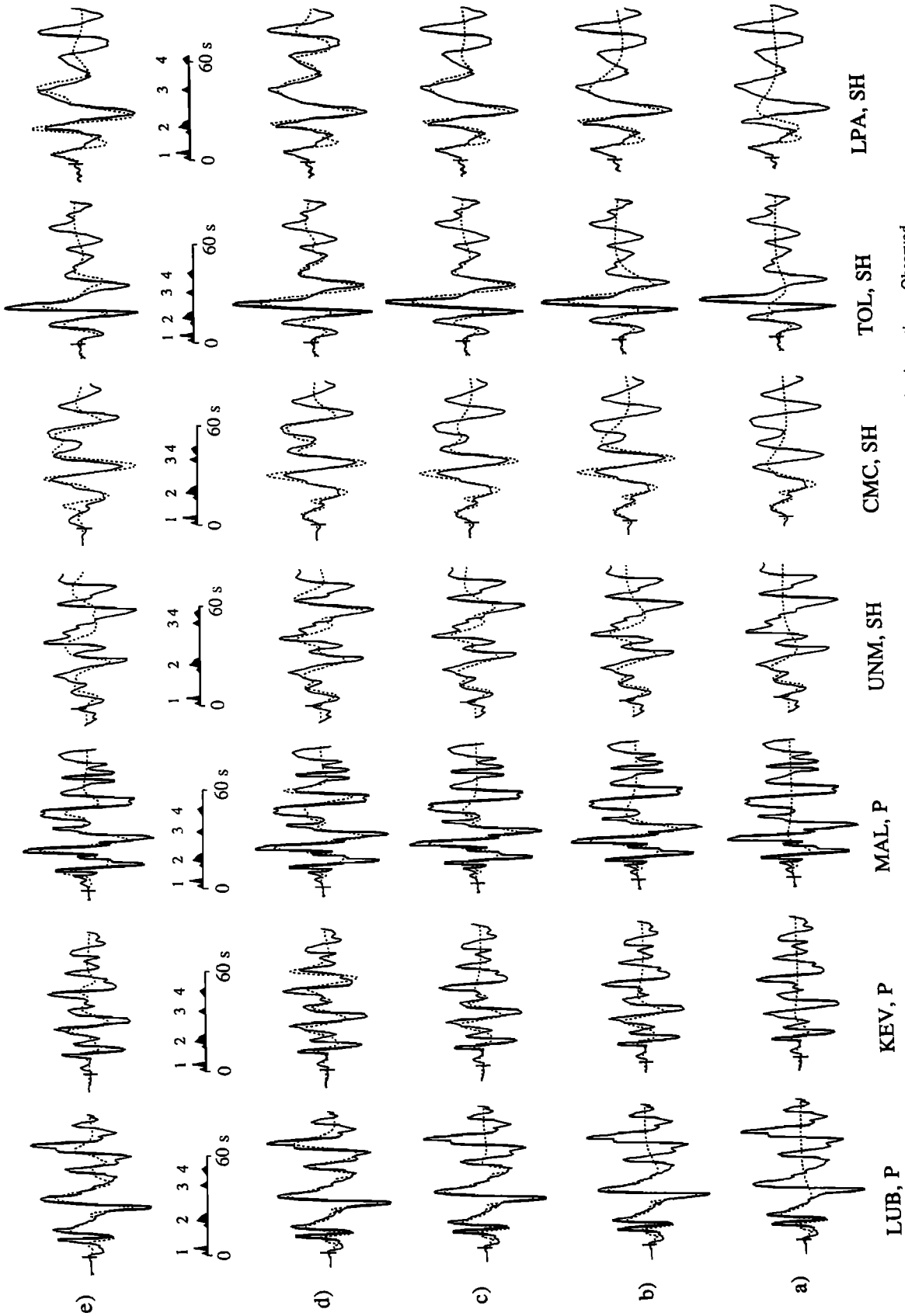
Fig. 10. Contribution of the four subevents forming the P and SH waveforms at different teleseismic stations. Observed seismograms are plotted with the solid lines and theoretical seismograms with the dashed lines. (a) The contribution of the first subevent. (b), (c), and (d) The effect of adding the succesive subevents to the synthetic waveforms. The synthetic waveforms in Figure 10d include all four subevents identified in the sequence. The apparent source time functions are shown on the time scale above the seismograms. (e) The waveforms for the best fitting unilaterally propagating source described in the caption of Figure 9.

TABLE 4. Source Parameters of the 1967 Caracas Earthquake Determined by Inversion of
Body Wave Seismograms

	Strike, deg	Dip, deg	Rake, deg	Depth, km	Moment, 10^{18} N m	Delay, s	Distance, km	Azimuth, deg	Duration, s
Subevent									
1	261	85	180	14.4	3.1	-	-	-	6
2	265	69	194	14.1	4.5	14.8	42	76	9
3	230	99	191	7.7	1.3	36.5	89	69	4
4	276	59	128	21.0	1.6	50.6	91	34	6
Average*	262	74	183	14.3	8.6	-	-	-	57

* Best double-couple of the moment tensor sum of the four subevents.

azimuth of 80°. This result substantiates formally the conclusion based on the visual inspection of waveforms that to the first order the predominant direction of rupture was eastward, approximately along the strike indicated by the average mechanism. The simple unilaterally propagating source model, however, did not produce completely satisfactory fit between the observed and synthetic seismograms at all stations (Figure 10e), indicating that a more complicated model involving precise positions and changes in mechanisms of subevents is necessary.

The final model was obtained in the following manner. Using the rough subdivision of the earthquake into subevents based on the first set of inversions, each subevent was analyzed independently by freeing the parameters pertaining to that subevent. For example, Figure 10a shows the results of inverting the time series within a time frame including only the first subevent. After the analysis of the first event was completed, the inversion scheme was applied to the next time window corresponding to the second subevent (Figure 10b). A similar stripping approach was followed sequentially for the
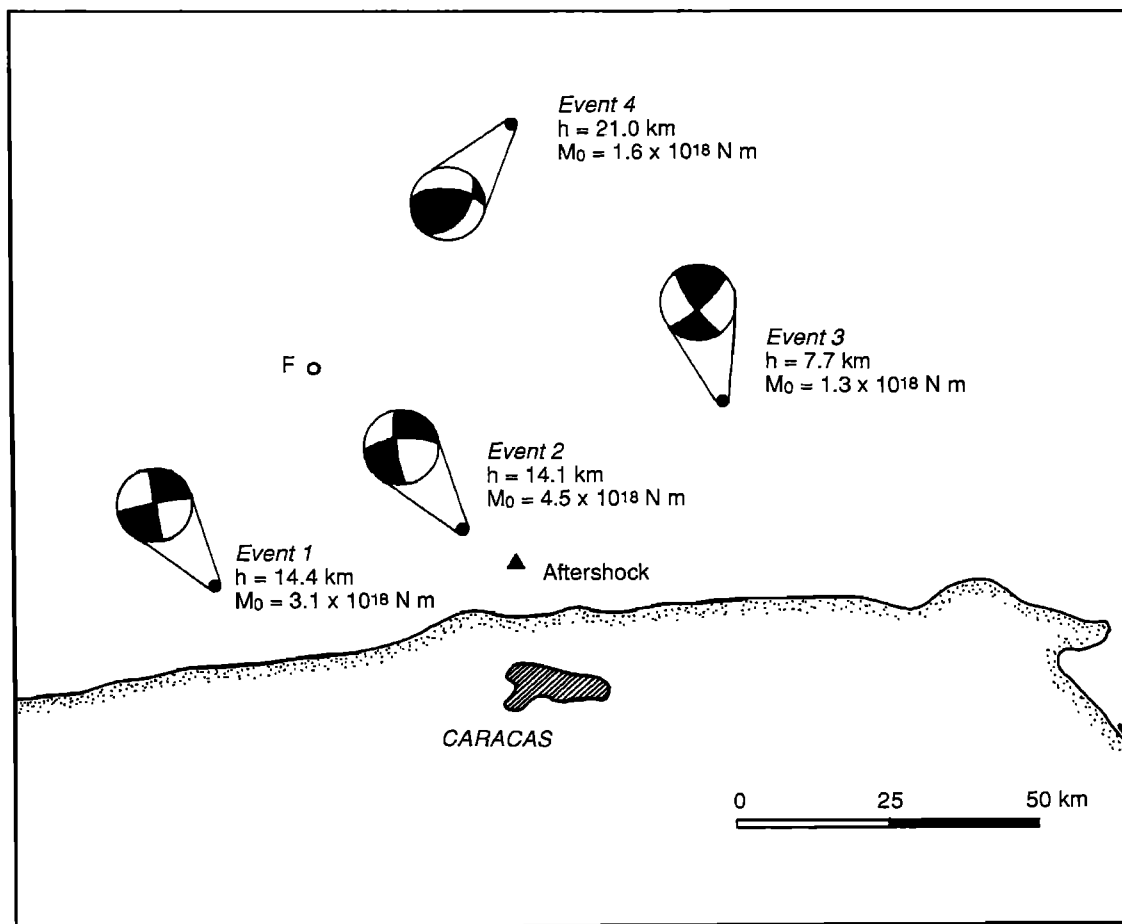

Fig. 11. The mechanism and location (solid circles) of the four subevents that form the Caracas earthquake. The mechanisms are plotted using a lower hemisphere stereographic projection, the dark quadrants representing compressional first motion. Solid triangle is the location of the relocated aftershock.

third and fourth subevents (Figures 10c and 10d). The resulting theoretical seismograms show now a better fit to the observed wave trains, most significantly for the later parts of the SH waves (Figure 10d). The inversion was not continued because at several stations the arrival of PP and ScS contaminates the records. In total, a timeframe of 65 s at each station was used in the inversion.

Once this piecewise inversion of the waveforms was finished, all parameters were freed, and the inversion was allowed to iterate to the best fitting solution. What was done by the stepwise inversion scheme described above was to find a stable and realistic starting model for the final inversion in which all parameters were allowed to vary at once. This minimized wild iterations and insured that the inversion algorithm would iterate to the true minimum in the residual space. The reason we were able to take this simplified approach is that the Caracas earthquake was composed of

distinct subevents well separated in time and because our main concern was to fit the major long-period arrivals in the observed waveforms.

A West-to-East Rupture Propagation

The final inversion yields for each subevent the seismic moment, focal mechanism, depth, source time function, and the location relative to the first subevent. We find that the main seismic radiation is dominated by four subevents (Table 4 and Figure 11). The first three events trigger sequentially from west to east, with distances of about 50 km from one another. These three events show almost pure strike-slip motion, although the mechanism of the third one begins to show some dip-slip component (Figure 11). The average depth of these three shocks is 14 km. The fourth event in the sequence is deeper, having a depth of 21 km, and it has a reverse-faulting mechanism with a small strike-slip component. The total
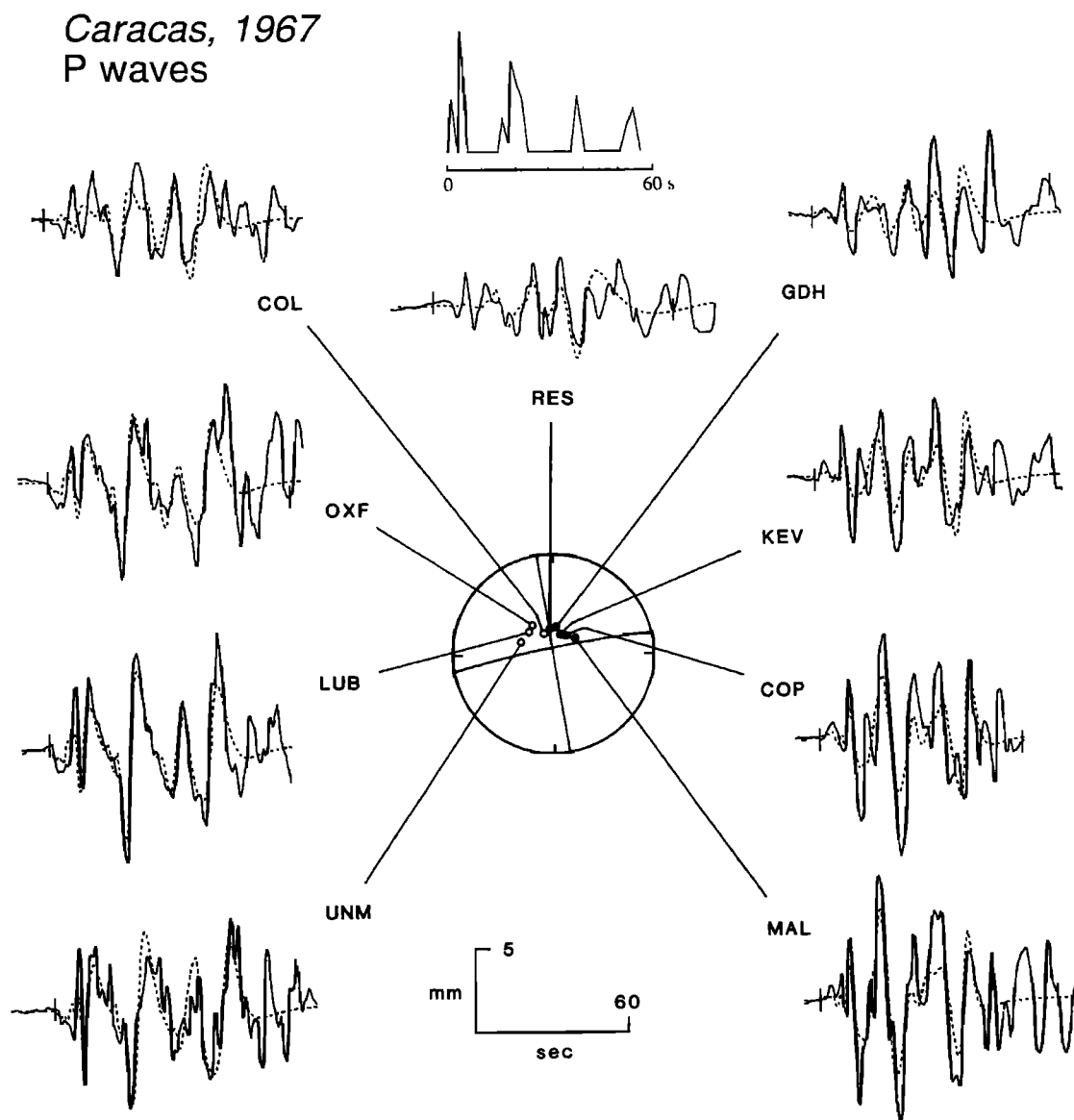

Fig. 12a. Comparison between the observed P waves (solid lines) and the theoretical seismograms (dashed lines) for the best fit model obtained by the simultaneous inversion of P and SH waves. The focal mechanism of the first subevent is shown in a lower hemisphere projection where the solid circles indicate compressions and the open circles dilatations. Amplitudes of the waveforms are normalized to an instrumental magnification of 1500 and a geometrical spreading corresponding to an epicentral distance of 40°.
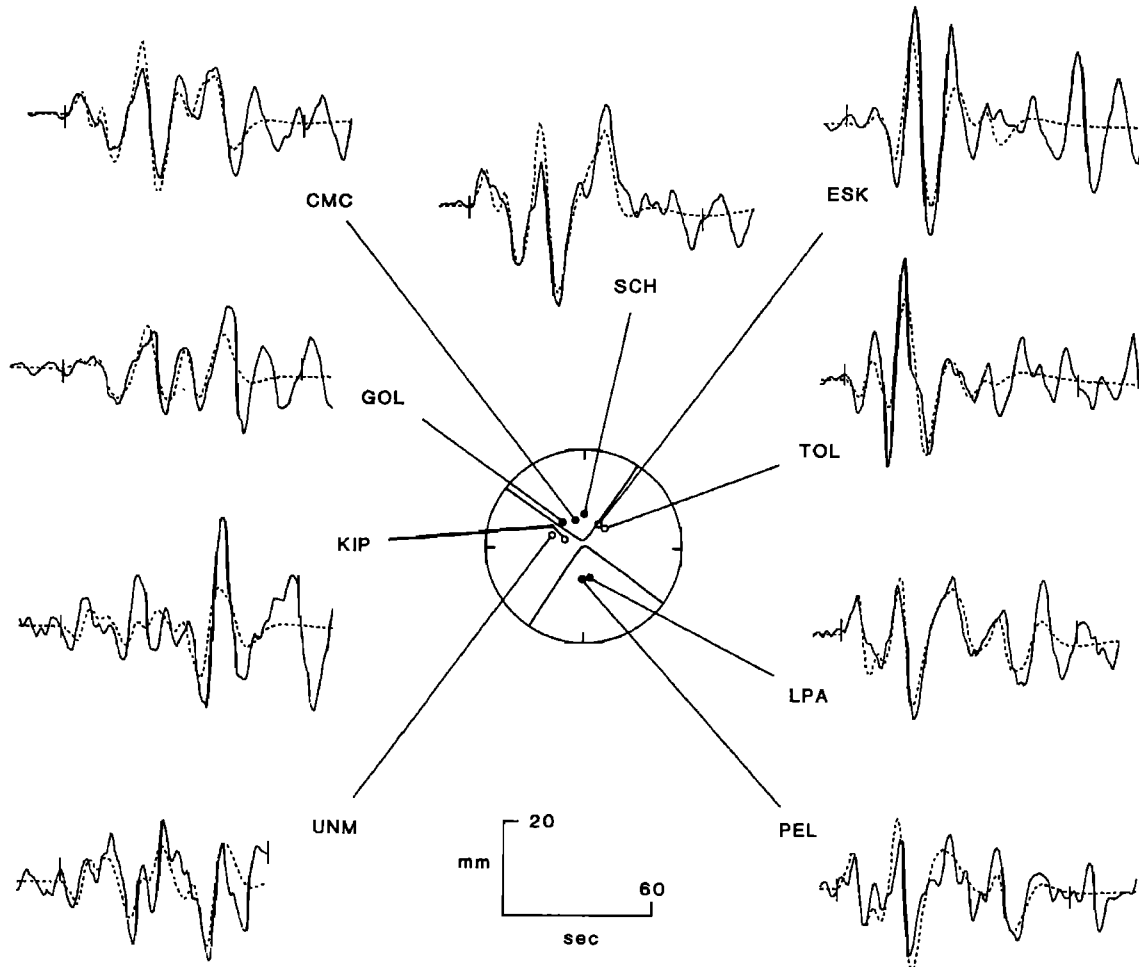
Caracas, 1967
SH waves

Fig. 12b. Comparison between the observed SH waves and the theoretical seismograms for the same inversion as in Figure 12a. The symbols and amplitude normalization are the same as for P waves.

seismic moment (tensor sum) of the Caracas earthquake is 8.6 × 10^{18} N m (M_w=6.6).

The orientation of the fault system defined by the locations of the subevents forming the Caracas earthquake is subparallel to the east-west oriented nodal plane of the fault plane solutions, indicating that the rupture occurred on an east-west oriented fault system. The synthetic seismograms computed using the source model derived from the joint inversion of P and SH waves agree well with the observed waveforms (Figures 12a and 12b). For all the stations analyzed, there are no significant mismatches in the arrival times of the major pulses between the observed and the synthetic waveforms. As expected, the matches are not as good for stations near the nodes of the radiation patterns, where small errors in the assumed ray takeoff angles produce large errors in shape and amplitudes of the arrivals. Also, due to the underparameterization of the source, the matches are better for the lower frequencies than for the higher frequencies. This is reflected in somewhat underestimated amplitudes of P waves in the direction of rupture. Overall, within a time frame of about 65 s from the onset of the body waves, the rupture process of the 1967 earthquake is well represented by the four shocks

(Figures 12a and 12b). Subevents 1 and 2 are the best resolved of the sequence. They are well separated in time and produce strong contributions on all seismograms (Figure 10). Subevent 4 is also well resolved. Due to its dip-slip mechanism, it has a stronger effect on the P waves than on the SH waves (Figure 10). The third subevent is partly buried in the coda of the first and second subevents and has the smallest effect on reducing the residuals; consequently, it is the least resolved subevent of the sequence.

In order to visualize the effect of the fault geometry on the body waves and to evaluate the resolution of the data, it is instructive to compare the solution obtained here with that determined by Rial [1978]. In the case of the P waves, the largest differences between the two source models occur in the western stations. For example, at station LUB (United States), the north-south trending fault model shows large phase offsets relative to the observations (Figure 13). SH waves are more sensitive to rupture propagation than P waves, and here the orientation of the fault system is even more crucial in fitting the observed seismograms. At stations UNM and TOL, neither the amplitude nor the phase of the synthetic seismograms produced with a north-south oriented fault match the

observations (Figure 13). This is particularly true for TOL, where the compressed nature of the observed *SH* waves cannot be matched by a fault system propagating north to south. The opposite is true at station UNM, where the synthetic seismogram for *Rial's* [1978] model is too short compared to the recorded *SH* wave. It should be pointed out that we were unable to reproduce the synthetic waveforms presented in Rial's paper using the parameters shown in his Table 1. Many of the synthetic waveforms presented by *Rial* [1978] appear to be missing the third subevent which he interpreted to be the largest one of all.

As we discussed before, stations located to the north and south of the fault zone do not exhibit large differences in the wave shapes, indicating they do not "see" a directivity effect in this direction. Our model matches both sets of stations well (Figure 13). *Rial* [1978], however, was not able to fit the later part of the *SH* wave at LPA, because the assumed directivity toward the south drastically compresses the seismogram. Rial suggested that the last part of the seismogram, which could not be matched by a north-south fault, was perhaps due to a coupled *PL* wave arriving "off-azimuth" after the *SH*. The source model derived here matches that part of the waveform at LPA (and PEL) without the need of invoking additional nonstandard waves (Figure 13). Many of the changes in waveform interpreted by *Rial* [1978] as being due to the directivity of the source are caused by the changes in focal mechanism of the third and fourth shocks. Notice that stations UNM, KIP and GOL, for example, lie very close to the nodal plane of the *SH* wave in the focal sphere (Figure 12*b*). Thus small changes in the focal mechanism show up as large variations in the amplitude and polarity of the radiated *SH* waves.

DISCUSSION OF RESULTS

Strike-Slip Faulting Along the Plate Margin

The results of the inversion presented here show that the Caracas earthquake occurred on the complex system of east-west trending faults that characterize the plate boundary in northern South America. The subevents composing the rupture are separated in space by distances much greater than the length of the individual faults, as inferred from the duration of their respective source time functions. The average duration of the source time function of each subevent indicates fault lengths shorter than about 12 km, whereas the average distance between the subevents is about 50 km. Thus the four shocks accounting for the main part of the radiated seismic energy rupture sequentially four different fault segments, instead of a single, long, or en echelon fault. No seismic energy appears to have been radiated in the segments between faults. This is indicative of a complex and severely faulted plate margin where the faults are highly stressed. The distances separating each subevent and the time delay among them suggest it was not stress concentration at the end of one fault rupture that triggered the next earthquake. Perhaps it was the passage of the surface waves that triggered this chain reaction of faulting.

It is interesting to point out that the great earthquake of 1812 that affected an elongated area along the Bocono fault from Caracas to Merida has been interpreted as consisting of two or more distinct events along the plate margin [*Kelleher et al.*, 1973]. This is suggested by the fact that several areas of very high intensity near the cities of Merida and Caracas, are separated by others showing only slight damage along the fault [*Centeno-Grau*, 1940; *Fiedler*, 1961; *Kelleher et al.*, 1973]. Complex earthquakes composed of several shocks breaking different fault segments may therefore be characteristic of this highly faulted plate boundary.

It is not possible to determine on which fault the individual shocks of the 1967 event occurred; offshore geology has not been mapped in this region of Venezuela. It appears that the sequence of events forming the Caracas earthquake took place on faults that are part of the Moron-La Victoria fault system (Figure 2), indicating that the relative plate motion between the Caribbean and the South American plates is accommodated

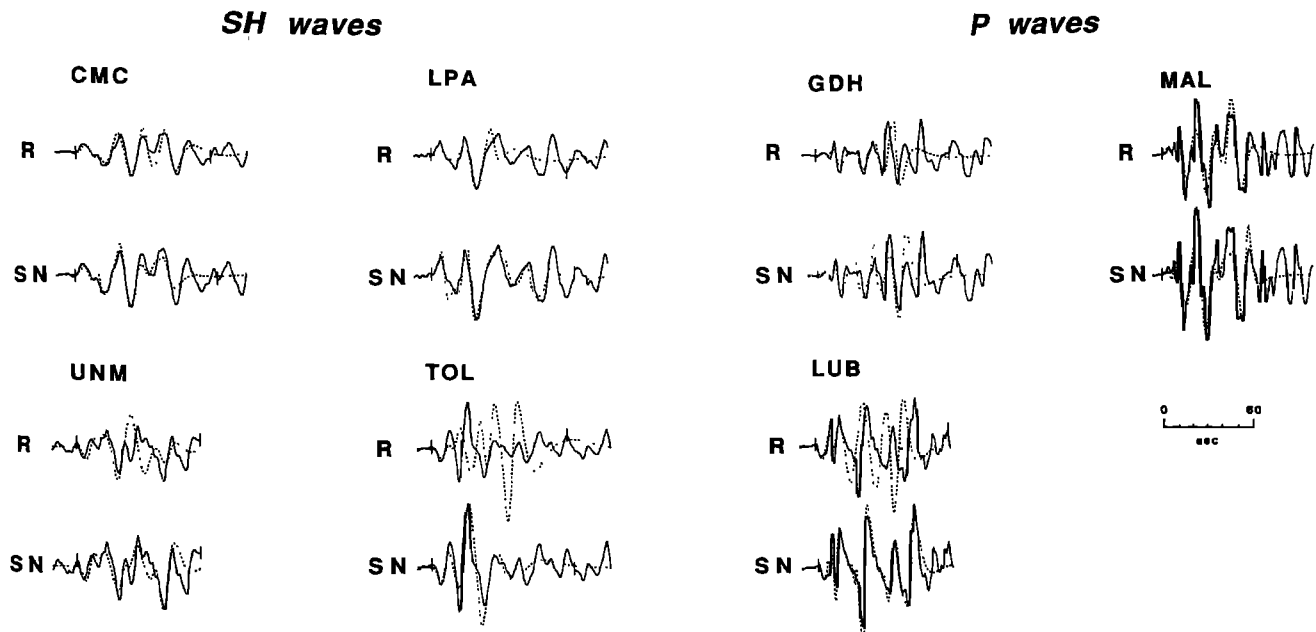## SH waves   P waves

Fig. 13. Comparison between the observed *P* and *SH* wave seismograms (solid lines) and theoretical seismograms (dashed lines) produced by the fault model suggested by *Rial* [1978] (R) and by the model proposed here (SN). Only several representative stations are shown. Because our moment estimate is different from Rial's, we compare only the wave shapes and not the absolute amplitudes; the amplitudes of the theoretical seismograms are scaled to match the power in the window of the observed waveform.

over a broad area of deformation, instead of being concentrated on a main through going fault.

The observation that in this segment of the plate boundary relative motion is accommodated over a large zone of deformation is not surprising, considering that the right-lateral strike slip faults defining the plate margin to the east and to the southwest undergo a sharp change in strike (Figure 1). The location of the 1967 earthquake is near the apex of the bend. The complex stress field due to the bend probably causes the complicated pattern of faulting observed in the north central coast of Venezuela, where faults of different type and orientation coexist with the dominant right-lateral strike-slip faults (Figure 2).

The important role played by fault bends in the initiation and and termination of faulting has been stressed before [e.g., Aki, 1979; King and Nábělek, 1985; Barka and Kadinsky-Cade, 1988]. The ruptures in individual earthquakes appear to be frequently limited to regions between bends in the fault trace, with bends acting as barriers to rupture propagation. This suggests that faulting initiated on the Bocono or on the Moron fault systems would not propagate around this curvature. Furthermore, the intense fault segmentation may also limit the largest possible size of an earthquake in the region near the bend.

Although the evidence presented here strongly suggests that the 1967 Caracas earthquake took place on a system of faults oriented east-west, the other conjugate faults mapped in the area are also probably seismogenic. In fact, the two relatively recent swarms in northcentral Venezuela, near towns of Los Teques (August 1986) and Ayagua (November 1980), appear to have occurred on NNW-SSE striking faults (anonymous reviewer, personal communication, 1989). This is a common mode of deformation in a complex tectonic environment. The recent Superstition Hills earthquake in southern California, for example, occurred on two conjugate faults [e.g., Budding and Sharp, 1988; Johnson, 1988; Hudnut et al., 1989]. Moreover, the 1968 Borrego Mountain earthquake, also in southern California, produced surface rupture along the main strand Coyote Creek fault, but the high seismic activity prior and after the earthquake occurred almost entirely on cross faults (M. Petersen et al., The interaction between secondary and master faults within the southern San Jacinto fault zone, manuscript in preparation, 1990). The NW to SE trending faults mapped in north central Venezuela (Figure 2) should be, therefore, considered when assessing the seismic hazard of this highly populated region.

Compressional Deformation in the Southern Caribbean

The epicenter of the fourth subevent lies about 100 km offshore of Caracas. The mechanism shows mainly reverse faulting at a depth of 21 km (Figure 11). This fourth shock is perhaps related to the compressional deformation observed in the Venezuela Basin basement beneath the Curaçao Ridge in the southern Caribbean [Talwani et al., 1977]. Seismic reflection records show evidence of folding in Quaternary sediments along the Curaçao Ridge and in the Los Roques Basin offshore Venezuela [Kellog and Bonini, 1982; Ladd et al., 1984; Silver et al., 1975; Talwani et al., 1977]. Case et al. [1984] have named this region, containing as much as 10 km of deformed pelagic and turbidite sediments of Neogene age, the Southern Caribbean Deformed Belt.

The poles of rotation proposed by Jordan [1975] and Stein et al. [1988] predict motion of the South American plate

relative to the Caribbean along an azimuth of about N75°W. The compression produced by this relative plate motion could account for this underthrusting. The reverse-faulting mechanism shown by the fault plane solution of the fourth subevent suggests compressional deformation induced by the thrust zone to the north. The depth obtained (21 km) would place the earthquake within the underthrust basement of the Venezuelan Basin, south of the Curaçao Trough.

Geometry of Faulting and Damage and Intensity Reports

The epicenter of the second subevent lies north of Caracas, about 12 km offshore. This subevent was the largest of the sequence (Table 4) with a magnitude of 6.4 (M_w). The relocated epicenter of the largest aftershock is less than 10 km away from this second subevent, suggesting that the aftershock may have occurred on the fault plane of the latter. The epicenter of the second subevent is very close to the area showing the highest intensities. It appears that the damage observed in Caracas and in neighboring coastal towns was produced mainly by this event and not by the three other events in the sequence which are over 50 km away from the area of largest damage.

More recently, Rial [1984] has argued that the Caracas Basin acts as a lens focusing seismic energy in the Palos Grandes area of Caracas, where several buildings collapsed [e.g., Whitman, 1969]. His results imply that this caustic is formed when the seismic waves approach the basin from the north. The second subevent in the series is located almost exactly to the north of Caracas and would be capable of causing the focusing effect suggested by Rial [1984] to partly explain the localized damage in Caracas. Whatever the case, it is clear Caracas sits on a highly faulted plate boundary, and the 1967 earthquake shows that even earthquakes with moderate magnitudes may produce intense localized damage.

SUMMARY

The Caracas earthquake of July 30, 1967, is one of the largest events to have occurred along the South American and Caribbean plate margin since the earthquake of 1900. The rupture process of the 1967 earthquake is complex. The formal inversion of the P and SH waveforms shows the source is composed of at least four subevents separated in time and space. The focal mechanism of the first three subevents indicate strike-slip faulting at an average depth of 14 km, consistent with the relative motion between the South American and Caribbean plates. These first three events are triggered sequentially from west to east, in a direction similar to the strike of the E-W trending nodal plane of the source mechanism. This fact strongly suggests that rupture took place on a system of faults oriented east-west.

The fourth event in the sequence shows reverse faulting at a depth of 21 km and appears to reflect compressional deformation along the southern margin of the Caribbean plate. Evidence for a compressive tectonic regime to the north is found in seismic reflection data showing underthrusting of the Caribbean plate beneath South America near the Curaçao Ridge and the associated deformation of Quaternary sediments in the Los Roques Basin.

The epicentral distances of aftershocks recorded in Caracas and the intensity data observed after the earthquake support the east-west orientation of the fault system derived from the inversion of body waves. Moreover, the relocated epicenter of the largest aftershock (m_b=4.4) that occurred 40 min after the main event lies within 10 km of the epicenter of the second

subevent of the mainshock. It appears that this large aftershock occurred on the same fault segment responsible for the second subevent. The second shock of the rupture sequence is about 12 km offshore, near the city of Caracas and the coastal towns that experienced the highest intensities. Therefore it appears that it was the second subevent of the Caracas earthquake which was mainly responsible for the damage.

The average separation of about 50 km between the subevents of the mainshock is much larger than the fault lengths inferred from the duration of the source time functions. This indicates that the Caracas earthquake ruptured several faults separated by a large distance and not adjacent or en echelon sections of a single fault. Each of these individual fault segments broke sequentially, perhaps triggered by the passage of the surface waves of the previous subevents.

The style of faulting during the earthquake suggests that the plate boundary near Caracas is complex, highly stressed, and very segmented. This geometry of faulting may be explained by the presence of a bend in the plate boundary, which changes from an east-west strike along the El Pilar fault system to a NE-SW strike along the Bocono fault zone. The intense fault segmentation may limit the largest possible size of an earthquake in the region of the bend. Although the Caracas earthquake of 1967 took place along faults oriented east-west, the possibility of moderately sized events occurring on conjugate faults oriented NW-SE should not be discounted in assessing the seismic hazard of the region.

REFERENCES

Aki, K., Characterization of barriers on an earthquake fault, *J. Geophys. Res., 84,* 6140– 6148, 1979.

Barazangi, M., and J. Dorman, World seismicity maps of ESSA, Coast and Geodetic Survey epicenter data for 1961–1967, *Bull. Seismol. Soc. Am., 59,* 369, 1969.

Barka, A. A., and K. Kadinsky-Cade, Strike-slip fault geometry in Turkey and its influence on earthquake activity, *Tectonics, 7,* 633–684, 1988.

Budding, K. E., and R. V. Sharp, Surface faulting associated with the Elmore Desert Ranch and Superstition Hills, California, earthquakes of 24 November 1987, *Seismol. Res. Lett., 59,* 49, 1988.

Burke, K., C. Cooper, J. F. Dewey, P. Mann, and J. L. Pindell, Caribbean tectonics and relative motions, *Mem. Geol. Soc. Am., 162,* 31–63, 1984.

Case, J. E., T. L. Holcombe, and R. G. Martin, Map of geologic provinces in the Caribbean region, *Mem. Geol. Soc. Am., 162,* 1–30, 1984.

Centeno-Grau, M., *Estudios Sismológicos,* 210–300 pp., Litografía del Comercio, Caracas, Venezuela, 1940.

Cisternas, A., and R. Gaulon, Síntesis sismotectónica del nordeste de Venezuela, *Rev. Geofís., 40,* 3–10, 1984.

Dewey, J. W., Seismicity studies with the method of joint hypocentral determination, Ph.D. thesis, Univ. of Calif., Berkeley, 1971.

Dewey, J. W., Seismicity and tectonics of western Venezuela, *Bull. Seismol. Soc. Am., 62,* 1711–1751, 1972.

Espinosa, A. F., and S. T. Algermissen, A study of soil amplification factors in earthquake damage areas, Caracas, Venezuela, *NOAA Tech. Rep. ERL, 280-ESL 31,* 1972.

Fiedler, G., Areas afectadas por terremotos en Venezuela, *Bol. Geol., 3,* 1791, 1961.

Fiedler, G., Estudio sismológico de la región de Caracas con relación al terremoto del 29 de julio de 1967, *Bol. Inst. Materiales Modelos Estracturales (IMME), VI* (23–24), 127–222, 1968.

García, D., and Y. P. Aggarwal, Seismotectonics of southern Venezuelan Andes, *Eos Trans. AGU, 63,* 1126, 1982.

Grasés, J., *Investigación Sobre los Sismos Destructores que Han Afectado el Centro y Occidente de Venezuela,* 3 vol., Informe INTEVEP, Caracas, Venezuela, 1980.

Hudnut, K. W., L. Seeber, and J. Pacheco, Cross-fault triggering in the November 1987 Superstition Hills earthquake sequence, southern California, *Geophys. Res. Lett., 16,* 199–202, 1989.

Johnson, C. E., Tectonic implications of the November 24, 1978 Superstition Hills earthquakes, Imperial Valley, CA, *Seismol. Res. Lett., 59,* 48, 1988.

Jordan, T. H, The present-day motions of the Caribbean plate, *J. Geophys. Res., 80,* 4433–4439, 1975.

Kelleher, J., L. R. Sykes, and J. Oliver, Possible criteria for predicting earthquake locations and their application to major plate boundaries of the Pacific and the Caribbean, *J. Geophys. Res., 78,* 2547–2585, 1973.

Kellog, J. N., and W. E. Bonini, Subduction of the Caribbean plate and basement uplifts in the overriding South American plate, *Tectonics, 1,* 251–276, 1982.

King, G., and J. Nábělek, Role of fault bends in the initiation and termination of rupture, *Science, 228,* 984–987, 1985.

Ladd, J. W., M. Truchan, M. Talwani, P. L. Stoffa, P. Buhl, R. Houtz, A. Mauffret, and G. Westbrook, Seismic reflection profiles across the southern margin of the Caribbean, *Mem. Geol. Soc. Am., 162,* 153–159, 1984.

Langston, C. A., and D. V. Helmberger, A procedure for modeling shallow dislocation sources, *Geophys. J. R. Astron. Soc., 42,* 117–130, 1975.

Minster, J. B., and T. H. Jordan, Present-day plate motions, *J. Geophys. Res., 83,* 5331–5334, 1978.

Molnar, P., and L. R. Sykes, Tectonics of the Caribbean and Middle American regions from focal mechanisms and seismicity, *Geol. Soc. Am. Bull., 80,* 1639–1689, 1969.

Nábělek, J. L., Determination of earthquake source parameters from inversion of body waves, Ph.D. thesis, 361 pp., Mass. Inst. of Technol., Cambridge, 1984.

Nábělek, J., Geometry and mechanism of faulting of the 1980 El Asnam, Algeria, earthquake from inversion of teleseismic body waves and comparison with field observations, *J. Geophys. Res., 90,* 12,713–12,728, 1985.

Nábělek, J., W.-P. Chen, and H. Ye, The Tangshan earthquake sequence and its implications for the evolution of the North China Basin, *J. Geophys. Res., 92,* 12,615–12,628, 1987.

Pérez, O. J., and Y. P. Aggarwal, Present-day tectonics of the southeastern Caribbean and northeastern Venezuela, *J. Geophys. Res., 86,* 10,791–10,804, 1981.

Rial, J. A., The Caracas, Venezuela earthquake of July 1967: A multiple source event, *J. Geophys. Res., 83,* 5405–5414, 1978.

Rial, J. A., Caustics and focusing produced by sedimentary basins: Applications of catastrophe theory to earthquake seismology, *Geophys. J. R. Astron. Soc., 79,* 923–938, 1984.

Richter, C. F., *Elementary Seismology,* 768 pp., W. H. Freeman, New York, 1958.

Rod, E., Strike slip faults of northern Venezuela, *Am. Assoc. Petr. Geol. Bull., 40,* 457–476, 1956.

Schubert, C., Are the Venezuelan fault systems part of the southern Caribbean plate boundary?, *Geol. Rundsch., 70,* 542–551, 1981.

Schubert, C., Basin formation along the Bocono-Moron-El Pilar fault system, Venezuela, *J. Geophys. Res., 89,* 5711–5718, 1984.

Schubert, C. and F. F. Krause, Moron fault zone, north-central Venezuelan borderland: Identification, definition, and neotectonic character, *Mar. Geophys. Res., 6,* 257–273, 1984.

Schubert, C., and C. Laredo, Late Pleistocene and Holocene faulting in Lake Valencia basin, north-central Venezuela, *Geology, 7,* 289–292, 1979.

Seed, H. B., I. M Idriss, and H. Dezfulian, Relationships between soil conditions and building damage in the Caracas earthquake of July 29, 1967, Univ. of Calif., *Rep. EERC70-2,* 201 pp., Berkeley, 1970.

Silver, E. A., J. E. Case, and H. J. MacGillavry, Geophysical study of the Venezuelan borderland, *Geol. Soc. Am. Bull., 86,* 213–226, 1975.